Proton-induced production of η on nuclei

L.-C. Liu
Isotope and Nuclear Chemistry Division, Los Alamos National Laboratory, Los Alamos, New Mexico 87544

J. T. Londergan and G. E. Walker
Department of Physics and Nuclear Theory Center, Indiana University, Bloomington, Indiana 47405
(Received 21 February 1989)

The features of the $(p,p'\eta)$ reaction are examined for incident proton energies between 0.8 and 1.6 GeV. Reactions are calculated for exclusive transitions in which the continuum proton and η are observed in coincidence. This process should be dominated by transitions $N+N\rightarrow N+N+\eta$ involving intermediate excitation of one of the nucleons to an $N(1535)$ isobar. We take phenomenological amplitudes for the process $\pi+N\rightarrow\eta+N$ in the nuclear medium. A theoretical formalism for the reaction amplitudes is derived and examined in detail. Nuclear distortions of the hadrons are estimated in the eikonal approximation. The theoretical cross sections are shown to be dominated by a single production amplitude. This results in the prediction that η production should occur entirely through $\Delta T=1$ non-normal parity nuclear transitions; i.e., that the nuclear states excited should show the spin-isospin characteristics of the exchanged meson. Peak reaction cross sections are predicted to have a strong dependence on the incident proton energy. Expected peak cross sections, for a target like ^{16}O, are on the order of 1 μb/sr^2 MeV.

I. INTRODUCTION

It is now possible to produce and detect η mesons at medium-energy machines such as Saturne or LAMPF. The η meson is a member of the pseudoscalar nonet with quantum numbers $J^\pi(I^G)=0^-(0^+)$. Unlike the pion, it is believed that the direct coupling of η mesons to nucleons is quite weak. For reasonably low energies, proton-induced η production from nuclei should be dominated by the amplitude $N+N\rightarrow N+N(1535)\rightarrow N+N+\eta$, where the $N(1535)$ is the S_{11} π-N resonance with $J^\pi=\frac{1}{2}^-$, and free width roughly 100 MeV.[1]

Experimental and theoretical studies of η production on nuclei are rather recent. Much of the impetus for such studies comes from two sources. First, theoretically Liu and Haider[2] have estimated the η-nucleus interaction. They have suggested that there may be quasibound η-nuclear states right at the threshold for η production. Second, a recent experimental measurement from Saturne of cross sections and tensor analyzing powers for the reaction $\mathbf{d}+p\rightarrow\eta+{}^3$He at threshold[3] have shown surprisingly large cross sections, with considerable structure. Laget and Lecolley have suggested[4] that this structure is evidence for extremely large many-body forces in η production.

In this paper, we have made theoretical predictions for proton-induced η production on nuclear targets. Experimentally, this would involve coincident detection of both the outgoing proton and η. We assume that the η is produced through the elementary process $\pi+N\rightarrow N(1535)\rightarrow\eta+N$, in which a virtual pion produces an intermediate isobar, the $N(1535)$, which then decays to η plus a nucleon. This is analogous to one process by which pions are produced in proton-induced reactions, through the intermediate formation of a $\Delta(1232)$. η production differs from pion production, in that the assumption of resonance domination in η production should be much more accurate than in the case of pion production, where nonresonant amplitudes are frequently appreciable.

In this paper, we estimate expected cross sections for η production by protons, leading to low-lying excited nuclear states. We sum the elementary η production amplitude over all active nucleons. We include distortions of the initial- and final-state hadrons through the eikonal approximation. We show that a single amplitude should dominate this process, and we calculate the magnitude of cross sections which could be expected for such reactions.

The reaction mechanism used in this paper simply sums up the contribution to η production from the elementary two-body amplitude $N+N\rightarrow N+N+\eta$, through intermediate $N(1535)$ states. Consequently, if many-body effects are extremely important, our predictions may dramatically underestimate the cross sections for η production. Similarly, we have not included any nuclear medium effects on the $N(1535)$ propagation; we discuss briefly the prospects for using reactions like this to obtain any information on the $N(1535)$ in the nuclear medium.

Our paper is organized in the following way: in Sec. II A, we review the elementary amplitude $N+N\rightarrow N+N+\eta$, through the $N(1535)$; in Sec. II B, we review the amplitudes for the reaction $A(p,p'\eta)A^*$ on a nucleus. We write down the amplitudes for this process in the plane-wave approximation (PWA); further expressions are given in the Appendix. In Sec. III A, we discuss our results for PWA cross sections for this reaction. In Sec. III B, we include nuclear distortions of the initial- and final-state hadrons via the eikonal approximation; we

present the formulas and show the results including distortion. Section IV gives conclusions and suggestions for future work in this area.

II. AMPLITUDES FOR THE $(N,N'\eta)$ REACTION

A. The $N+N\rightarrow N+N+\eta$ reaction

In order to estimate cross sections for production of η mesons from nuclei, we need to make assumptions regarding the process by which η mesons are produced in nuclear collisions; that is, we require amplitudes for the process $N+N\rightarrow N+N+\eta$ in the nucleus. At the energies of interest in this paper, we are not far above the η-production threshold. Consequently, η production should be dominated by formation of the $N(1535)$ isobar; i.e., the η should be produced through the process

$$N+N\rightarrow N^*(1535)+N\rightarrow\eta+N+N\ . \tag{1}$$

In Eq. (1), $N^*(1535)$ is the π-N S_{11} resonance, having $l=0$, $J^\pi=\frac{1}{2}^-$, and isospin $\frac{1}{2}$ [in the latest particle data tables,[1] this particle is the $N(1535)$. We frequently refer to it as $N^*(1535)$, in order to differentiate it easily from the nucleon]. We assume that the $N(1535)$ isobar is produced by a virtual meson exchange between the nucleons; this virtual meson excites one of the nucleons to an isobar, which then decays to an η plus a nucleon. This process is shown schematically in Fig. 1. In this paper we will restrict our attention to virtual pions, although there is some evidence that the ρ meson may also contribute to this process.[5] We then need to evaluate the process

$$\pi+N\rightarrow N^*(1535)\rightarrow\eta+N \tag{2}$$

for virtual pions.

We can obtain the amplitude of Eq. (2) for η production by assuming the form of interaction Lagrangians for the coupling of mesons to a nucleon or isobar

$$\begin{aligned}\mathcal{L}_{\rm int}^{NN\pi}&=\frac{f_\pi}{m_\pi}\bar{\psi}_N\gamma^\mu\gamma^5\boldsymbol{\tau}\psi_N\cdot\partial_\mu\boldsymbol{\phi}_\pi\ ,\\ \mathcal{L}_{\rm int}^{N^*N\pi}&=f^*\bar{\psi}_{N^*}\boldsymbol{\tau}\psi_N\cdot\boldsymbol{\phi}_\pi\ ,\\ \mathcal{L}_{\rm int}^{N^*N\eta}&=f_\eta\bar{\psi}_{N^*}\psi_N\phi_\eta\ .\end{aligned} \tag{3}$$

In Eq. (3), ψ_N (ψ_{N^*}) represents the nucleon (isobar) fields, and ϕ_π (ϕ_η) is the pion (eta) field. In Ref. 6, the η-production amplitude was assumed to be of the form

$$\langle p'|t_{\pi N\rightarrow\eta N}(W)|p\rangle=\frac{g_{N^*N\pi}g_{N^*N\eta}}{\sqrt{2W}}\frac{h_\eta(p')h^*(p)}{W-M^0-\Sigma(W)}\ . \tag{4}$$

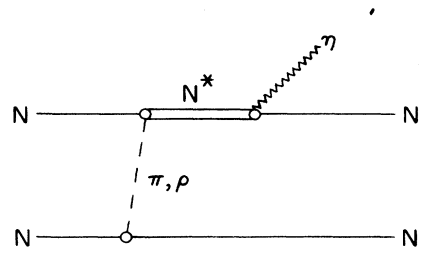

FIG. 1. Elementary amplitude for the reaction $N+N\rightarrow N+N+\eta$.

In Eq. (4), $g_{N^*N\pi}$ and $g_{N^*N\eta}$ are the coupling constants from ref. 6 and W is the interaction energy in the meson-nucleon c.m. frame. The coupling constants adopted in this work are related to those given in Ref. 6 by

$$f^*f_\eta\equiv 2\pi^2\left[\frac{\omega_\pi\omega_\eta}{3W^2}\right]^{1/2}g_{N^*N\pi}g_{N^*N\eta}\ , \tag{5}$$

where ω_π (ω_η) is the pion (eta) energy. Following Ref. 6, we assume

$$\begin{aligned}&f_\pi^2/4\pi=0.081\ ,\\ &g_{N^*N\pi}=1.301\ ,\\ &g_{N^*N\eta}=0.769\ .\end{aligned} \tag{6}$$

The isobar form factors are defined by

$$h(k)=\Lambda^2/(\Lambda^2-|\mathbf{k}|^2)\ , \tag{7}$$

consistent with Bhalerao and Liu.[6] For the $NN\pi$ vertex, we used form factors which depended on the four-momentum transfer at the meson vertex

$$h_\pi(k,\omega)=\frac{\Lambda^2-m_\pi^2}{\Lambda^2-\omega^2+|\mathbf{k}|^2}\ , \tag{8}$$

as in Ref. 7. We used the value $\Lambda=1200$ MeV/c for all form factors.

In Ref. 6, the coupling constants and form factors were determined from the π-N phase shifts in the S_{11} channel through a coupled-channel approach. η-production amplitudes were also determined for processes involving higher N^* resonances. This parametrization fit both the π-N phase shifts[8] and experimental cross sections for $\pi^-+p\rightarrow\eta+n$.[9] For the energies of interest in this paper, η production should be completely dominated by the $N^*(1535)$ resonance.

M^0 and $\Sigma(W)$ in Eq. (4) denote, respectively, the bare mass and (energy-dependent) self-energy for the isobar. In the elementary η-production interaction, the latter quantity takes into account both the dispersive effects and inelasticities arising from couplings among the πN, $\pi\pi N$, and ηN channels. In this paper, we have neglected the self-energy effects; that is, we approximated $M^0+\Sigma(W)=M_{N^*}-i\Gamma/2$, and we used the physical values $M_{N^*}=1535$ MeV and $\Gamma=100$ MeV. This should be a good approximation for the $(p,p'\eta)$ reaction, since we can select the final kinematics to make the final-state η-p system centered around the $N^*(1535)$ resonance.

In our calculations, we have used a nonrelativistic reduction of the amplitudes. As a result, we have replaced the $NN\pi$ vertex with its nonrelativistic reduction

$$\mathcal{L}_{\rm int}^{NN\pi}=\frac{f_\pi}{m_\pi}\bar{\chi}_N\boldsymbol{\sigma}\cdot\mathbf{q}\boldsymbol{\tau}\chi_N\cdot\boldsymbol{\phi}_\pi\ ; \tag{9}$$

in Eq. (9), the χ_N represent two-component nucleon spinors, coupled to a pion with momentum q.

B. Amplitudes for η production

We assume that the η is produced via a virtual $N(1535)$ isobar. A virtual pion excites a nucleon to an isobar, which then decays to an η and a nucleon. In this section, we will neglect the initial- and final-state interactions of the hadrons with the nucleus. Such distortion effects will be included in Sec. III B.

The four amplitudes which we have studied for proton-induced η production are shown in Fig. 2. We include four distinct amplitudes in our calculation. The first (A), shown in Fig. 2(a), represents excitation of the projectile proton to $N(1535)$ by a virtual pion; this isobar propagates and decays to a continuum proton plus the η meson. The second (B), shown in Fig. 2(b), represents excitation of a target proton to the $N(1535)$; this then decays to a continuum proton plus η. The third and fourth amplitudes, C and D [Figs. 2(c) and 2(d), respectively], are obtained from A and B, respectively, by exchanging the two final nucleon lines.

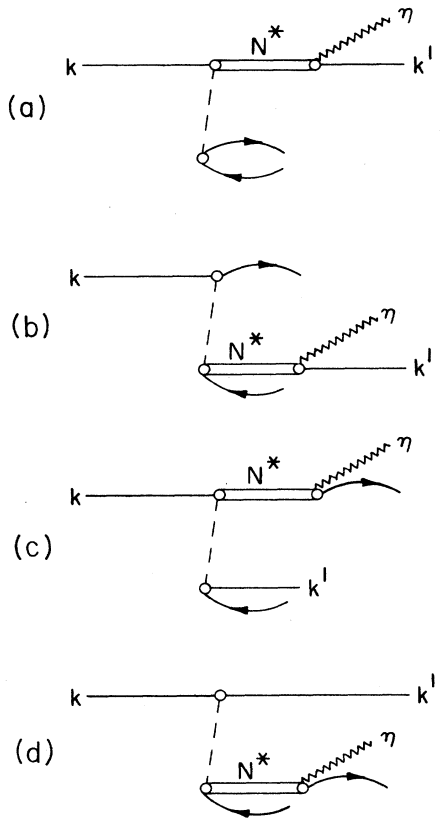

FIG. 2. Amplitudes considered for the $(p,p'\eta)$ reaction. (a) A, "projectile excitation" amplitude: incident proton with momentum $\mathbf{k}$ interacts with target nucleon via intermediate pion, exciting proton to an $N^*(1535)$ isobar, which then decays to proton with momentum $\mathbf{k}'$, and η; (b) B, "target excitation" amplitude: target proton is excited to isobar. This amplitude is identical to A except that projectile and target protons in the initial state are interchanged; (c) C, projectile is excited to $N^*(1535)$ isobar. This amplitude is similar to A except that the final-state nucleons are interchanged; (d) D, target nucleon is excited to $N^*(1535)$, which decays to η plus nucleon. This amplitude is identical to C if the projectile and target nucleons in the initial state are interchanged.

In this calculation, we have not included the "crossed" graphs, where the order of the pion and η lines is interchanged. This is because the crossed graphs were not included in the initial amplitudes of Bhalerao and Liu;[6] thus, the coupling constants obtained in that paper may be thought of as *effective* coupling constants when only the direct amplitude for η production is included. If we were to include the crossed graphs, for consistency we would have to refit the coupling constants and form factors. In Sec. III A, we have included the crossed graphs for the dominant amplitude (although we have not refit the coupling constants and form factors in the elementary amplitude); we find that inclusion of the crossed graphs makes almost no change in our final results, which gives an *a posteriori* justification for neglecting these terms.

The amplitude of Fig. 2(a), or "amplitude A," corresponds to emission of a virtual pion from a target nucleon, excitation of the incident proton to $N(1535)$, with subsequent decay to a continuum proton and pion; thus, we refer to this amplitude as the "projectile excitation" term. For amplitude A the plane-wave amplitude has the form

$$T_A = c_\tau \rho_{fi}^{\sigma\tau}(\mathbf{q}_A)\frac{f_\pi f^* f_\eta}{m_\pi} H(q_A)\frac{1}{D^*(q_A^*,\omega_A^*)D_\pi(q_A,\omega_A)}\ , \tag{10}$$

where

$$\begin{aligned} &\mathbf{q}_A = \mathbf{k}_\eta + \mathbf{k}' - \mathbf{k},\quad \omega_A = \epsilon_f - \epsilon_i \approx 0\ , \\ &\mathbf{q}_A^* = \mathbf{k}_\eta + \mathbf{k}',\quad \omega_A^* = E' + E_\eta\ . \end{aligned} \tag{11}$$

In Eq. (10), the coupling constants f represent the "bare" coupling constants of Eq. (6); the form factors are absorbed in the factor

$$H(q_A) = h_\pi(q_A,0)h^*(q_A)h_\eta(k_\eta)\ ,$$

where the form factors h are given in Eqs. (7) and (8). D^* represents the free propagator for the intermediate isobar as discussed in Eq. (4), and D_π is the propagator for the pion exchanged between the projectile and target nucleons. The incident and final proton states are denoted by k and k', and the initial and final bound nucleons are denoted by i and f, respectively. The fourth component of the virtual meson momentum, ω_A, is given by the difference in energy between the initial and final nuclear states. Because of the large energy necessary to create the η, this is inherently a high-momentum-transfer process. We will be examining transitions to low-lying nuclear states; in comparison with the three-momentum q_A of the virtual pion, ω_A can be neglected. Inclusion of ω_A would not change our results significantly, even for nu-

clear excitations as high as 100 MeV.

The spin-isospin transition matrix $\rho^{\sigma\tau}$ in Eq. (10) is given by

$$\rho_{fi}^{\sigma\tau}(\mathbf{q})=\left\langle f\left|\sum_j \boldsymbol{\sigma}_j\cdot\mathbf{q}\tau_j\right|i\right\rangle , \tag{12}$$

where the initial and final nuclear states are denoted by i and f, respectively, and the sum is over all target nucleons. For this paper we will consider cases where the final state is a single particle-hole state relative to the initial state, and we assume that the core is inert, in which case Eq. (12) can be written

$$\rho_{fi}^{\sigma\tau}(\mathbf{q})=\langle\phi_f|\boldsymbol{\sigma}\cdot\mathbf{q}|\phi_i\rangle . \tag{13}$$

In Eq. (13), only a single "active" nucleon contributes to the transition density. The isospin operator for the $(p,p'\eta)$ reaction can then be absorbed into a single overall factor c_τ, which depends on the isospin of the final nuclear state. Assuming that the initial nuclear state has isospin zero, then $c_\tau=-\sqrt{2}$ for final isospin 1, and $c_\tau=0$ for final isospin 0. Thus, amplitude A corresponds to non-normal-parity $\Delta T=1$ nuclear transitions. For the projectile excitation amplitude, the nuclear transitions have the characteristic spin and isospin of the exchanged meson. Thus this statement would not change if we also included ρ meson exchange.

In this paper, our aim is to explore the qualitative features of the $(p,p'\eta)$ reaction. Therefore, we have used simple Gaussian forms for the single-particle transition densities and wave functions,

$$\phi(p)=\left[\frac{4\pi}{p_0^2}\right]^{3/4}\exp(-p^2/2p_0^2) , \tag{14}$$

$$\rho(p)=\exp(-p^2/4p_0^2) . \tag{15}$$

The model wave functions thus depend upon a single momentum scale, p_0. This parameter has been fixed by requiring that it reproduce the same mean-squared single-particle momentum seen in electron scattering data. In terms of the Fermi momentum, p_0 then obeys the relation

$$p_0^2=\tfrac{2}{3}\langle p^2\rangle=\tfrac{2}{5}k_F^2 . \tag{16}$$

These nuclear wave functions are oversimplified and lack the dependence on orbital and spin degrees of freedom. They reproduce single-particle momentum distributions for the nucleus as a whole, rather than being typical of a particular shell. Also, they fall off too fast for large momentum and are structureless, lacking the deep minima frequently found in realistic nuclear transition densities. These features have been discussed in detail in Ref. 7.

As was discussed in Eq. (4), the isobar propagator is given by the free isobar pole term with no medium modification of the position or width. In the paper examining the $(p,p'\pi)$ reaction,[7] a pion-nucleus optical potential and spreading width were used from isobar-hole calculations[10] to estimate medium effects on the virtual $\Delta(1232)$. The parameters of this potential were determined from fits to the existing extensive π-nucleus elastic cross sections in the Δ resonance region. However, because of the paucity of data on η-nuclear reactions, it would be virtually impossible to pin down those parameters necessary to estimate medium effects on the intermediate $N^*(1535)$. The resulting uncertainty on the position and width of the N^* in the nuclear medium should have no effect on the basic results of the present study, as the η distortions based on the theoretical amplitudes of Ref. 6 predict a rather weak η-nucleus interaction.

The pion propagator in our work is given by

$$D_\pi(\mathbf{q},\omega)=[\omega^2-\mathbf{q}^2-m_\pi^2-\Pi(\mathbf{q},\omega)+i\epsilon]^{-1} , \tag{17}$$

for the pion, where Π is the self-energy of the pion with momentum q and energy ω. The pion self-energy has been calculated by summing particle-hole and Δ-hole ring diagrams for a pion in a Fermi gas with Fermi momentum appropriate for ^{16}O. Equations for the pion self-energy are given in Ref. 7.

The second amplitude considered in this model corresponds to emission of a virtual meson by the projectile proton, as shown in Fig. 2(b). This meson excites a target nucleon to an $N(1535)$, which then decays to the final continuum proton and η. We refer to this amplitude as the "target excitation" term (or "amplitude B"). This amplitude has the form

$$T_B=c'_\tau\frac{f_\pi f^* f_\eta}{m_\pi}\int\frac{d\mathbf{q}}{(2\pi)^3}\frac{H_B(q)\phi_f^\dagger(\mathbf{k}-\mathbf{q})\phi_i(\mathbf{k}'+\mathbf{k}_\eta-\mathbf{q})}{D^*(q_B^*,\omega_B^*)D_\pi(q,\omega_B)}\times\langle f|\boldsymbol{\sigma}\cdot\mathbf{q}|k\rangle , \tag{18}$$

where

$$\begin{aligned}\omega_B&=T_p+\epsilon_f\approx T_p ,\\ \mathbf{q}_B^*&=\mathbf{k}'+\mathbf{k}_\eta=\mathbf{q}_A^* ,\\ \omega_B^*&=E'+E_\eta=\omega_A^* .\end{aligned} \tag{19}$$

This amplitude is proportional to the product of two single-particle wave functions, integrated over the momentum $\mathbf{q}$. As this term is nonlocal, it cannot be written in terms of a local spin-isospin transition density, but it requires a nonlocal density matrix. In this term, we have neglected the contribution of the single-particle binding energy to the energy ω_B carried by the virtual meson. In Eq. (18), the isospin coefficient $c'_\tau=1/\sqrt{2}$ for $T=1$ final nuclear states, and $-3/\sqrt{2}$ for $T=0$ nuclear states. The form factor is given by

$$H_B(q)=h_\pi(q,\omega_B)h^*(q)h_\eta(k_\eta) .$$

The "target excitation" amplitude is obtained from the "projectile excitation" term by interchanging the projectile and target nucleon lines in Fig. 1(a). All of the additional terms in our amplitude are obtained from the amplitude of Fig. 2(a) by interchanging either the initial- or final-state nucleon lines.

The third amplitude, given in Fig. 2(c), is obtained from amplitude A by exchanging the continuum and bound nucleon lines in the final state. We refer to this term as "amplitude C;" it has the form

$$T_C = c'_\tau \frac{f_\pi f^* f_\eta}{m_\pi} \int \frac{d\mathbf{q}}{(2\pi)^3} \frac{H_C(q)\phi_f^\dagger(\mathbf{k}-\mathbf{k}_\eta-\mathbf{q})\phi_i(\mathbf{k}'-\mathbf{q})}{D^*(q_C^*,\omega_C^*)D_\pi(q,\omega_C)} \times \langle k'|\boldsymbol{\sigma}\cdot\mathbf{q}|i\rangle \ , \tag{20}$$

where

$$\begin{aligned} &\omega_C = -\epsilon_i - T_{p'} \approx -T_{p'} \ , \\ &\mathbf{q}_C^* \approx \mathbf{k}_\eta \ , \\ &\omega_C^* \approx E_\eta + M_p \ . \end{aligned} \tag{21}$$

In Eq. (20), several approximations in kinematics have been made. Small bound-state energies and momenta have been dropped in Eq. (21). This simplication allows us to take the isobar propagator outside the integral over $\mathbf{q}$. The form factor

$$H_C(q) = h_\pi(q,\omega_C)h^*(q)h_\eta(k_\eta) \ .$$

Like amplitude B, this amplitude is also proportional to a transition density matrix operator.

The final amplitude is obtained by exchanging the bound and continuum nucleon lines in the final state of the target excitation amplitude. This term is shown in Fig. 2(d). We refer to this term as "amplitude D," and it has the form

$$T_D = c_\tau \frac{f_\pi f^* f_\eta}{m_\pi} H(q_D) \frac{\tilde{\rho}_{fi}}{D^*(q_D^*,\omega_D^*)D_\pi(q_D,\omega_D)} \ , \tag{22}$$

where

$$\begin{aligned} &\mathbf{q}_D = \mathbf{k}' - \mathbf{k} \ , \\ &\omega_D = T_{p'} - T_p \ , \\ &\mathbf{q}_D^* \approx \mathbf{k}_\eta \ , \\ &\omega_D^* \approx E_\eta + M_p \ . \end{aligned} \tag{23}$$

In Eq. (23) the same approximations were made as in Eq. (21). The form factor

$$H(q_D) = h_\pi(q_D,\omega_D)h^*(q_D)h_\eta(k_\eta) \ .$$

This amplitude, like the projectile excitation amplitude, is proportional to a nuclear transition density;

$$\tilde{\rho}_{fi} \equiv \rho(-\mathbf{q}_A)\langle k'|\boldsymbol{\sigma}\cdot\mathbf{q}_D|k\rangle \ , \tag{24}$$

where $\mathbf{q}_A$ is given in Eq. (11) and ρ is given in Eq. (15).

The c.m. differential cross section is given in terms of the above amplitudes as

$$\frac{d^3\sigma}{d\Omega' d\Omega_\eta dE'} = \frac{10^4}{2(2\pi)^5} \frac{k' k_\eta E' E}{k(1+E/E_A)} |T_{fi}|^2 \ . \tag{25}$$

In Eq. (25), the units are μb/sr^2 MeV, and $|T_{fi}|^2$ is obtained by squaring the sum of the amplitudes of Eqs. (10), (18), (20), and (22); averaging over initial spins; and summing over final spins. With our approximations for the momentum dependence of the isobar propagator, and with the simple Gaussian wave functions and transition densities which we have employed, then the PWA cross sections can be reduced to a sum of terms requiring no more than a single integral. The form of the final plane-wave equations, and the expressions which were integrated, are listed for completeness in the Appendix.

III. RESULTS AND DISCUSSION

A. General features of reaction amplitudes

We have calculated the η-production cross sections in coplanar geometry, where the incident and outgoing particles all lie in a plane. All results are shown in the c.m. system. We have kept the angle between the incident and outgoing protons fixed at $-10°$ relative to the incident direction [angles are negative (positive) if they occur to the right (left) of the incident beam direction, looking down on the reaction plane]. The kinematics have been shown for a target with mass $A = 16$.

In Fig. 3, we show the differential cross sections for $(p,p'\eta)$, in plane-wave approximation, as a function of the angle θ_η for incident proton kinetic energies 1.0, 1.3,

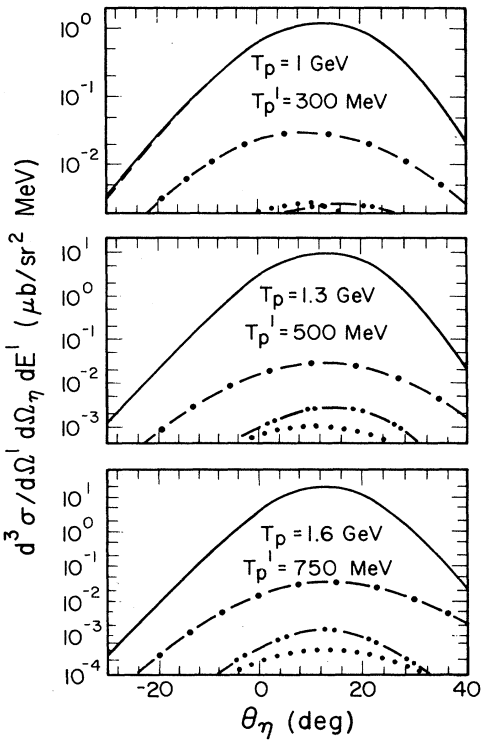

FIG. 3. Differential cross sections, in μb/sr^2 MeV, vs c.m. angle θ_η for the outgoing η. The outgoing proton angle is fixed at $\theta' = -10°$. (a) Incident proton energy 1.0 GeV, and outgoing proton kinetic energy $T_{p'} = 300$ MeV; (b) incident energy 1.3 GeV and $T_{p'} = 500$ MeV; (c) incident energy 1.6 GeV and $T_{p'} = 750$ MeV. Solid curve, full differential cross section; dashed curve, result using only amplitude A of Fig. 2; dot-dot-dashed curve, result using amplitude B; dotted curve, result using only amplitude C; dot-dashed curve, result using only amplitude D of Fig. 2. Results are shown in PWA.

and 1.6 GeV, for fixed outgoing proton kinetic energy. At each incident energy, the outgoing proton kinetic energy corresponds to the maximum cross section for that incident energy.

In Fig. 4, we show the η production cross section for fixed η angle, as a function of the outgoing proton kinetic energy $T_{p'}$. Cross sections are shown for incident proton energies 1.0, 1.3, and 1.6 GeV; the η angle is fixed at $+10°$, which gives the maximum cross sections for this reaction for each incident energy. In contrast to the cross sections versus η angle of Fig. 3, which showed a rather sharp peak in the cross section, the peak cross section in Fig. 4 is rather broad, extending over a wide range of $T_{p'}$.

We see that the peak cross section increases rather dramatically with the incident proton energy. In Fig. 3, the peak PWA cross sections are roughly 1, 10, and 30 μb/sr^2 MeV at 1.0, 1.3, and 1.6 GeV, respectively. This occurs because the minimum momentum transfer to the nucleus *decreases* as the incident proton energy *increases*. This is shown in Fig. 5, which plots the momentum transfer to the nucleus versus outgoing proton kinetic energy, for fixed outgoing proton and η angles of $-10°$ and $+10°$, respectively.

The curves show that the nuclear momentum transfer

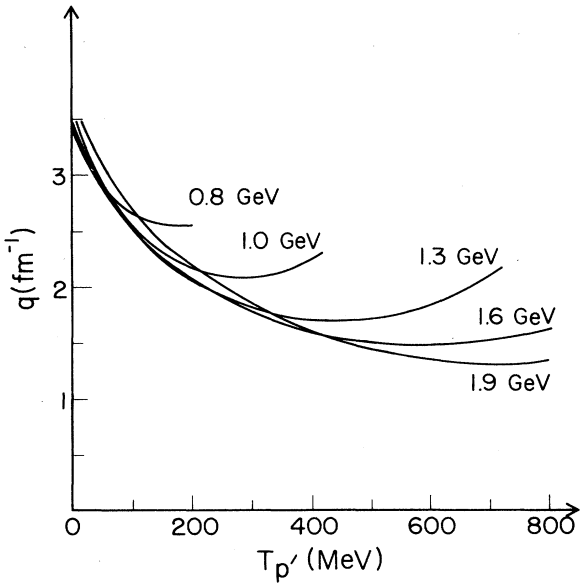

FIG. 5. Momentum transfer to the nucleus, in fm^{-1}, vs outgoing proton kinetic energy $T_{p'}$, for various incident proton energies. Outgoing proton and η angles are fixed at $-10°$ and $+10°$, respectively.

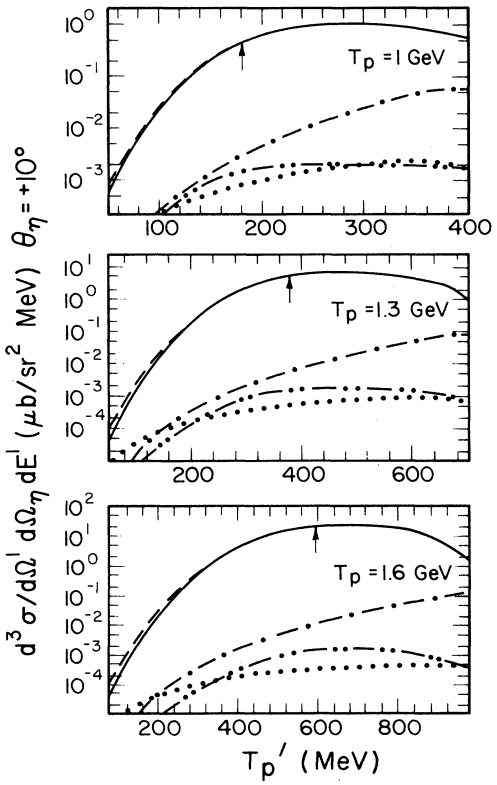

FIG. 4. Differential cross sections vs outgoing proton kinetic energy $T_{p'}$, with c.m. angle θ_η fixed at $+10°$. (a) Incident proton kinetic energy 1.0 GeV; (b) incident energy 1.3 GeV; (c) incident energy 1.6 GeV. All other conditions are the same as for Fig. 3. Arrows denote kinematics corresponding to the peak of the $N(1535)$ resonance.

decreases markedly as the incident proton energy increases. η production is inherently a high-momentum-transfer process; peaks in the cross sections occur at the lowest possible momentum transfers. To show this, in Fig. 4 we have placed arrows at those positions where the outgoing particle kinematics are directly centered on the $N^*(1535)$ resonance. The peaks of the cross sections do not occur at this position; this shows that minimizing the momentum transfer is more important than achieving the resonant kinematics for these exclusive reactions.

The solid curve in Fig. 3 gives the full PWA cross section. The dashed and dotted curves give the cross section for each of the four amplitudes separately. It can immediately be seen that the cross section is dominated by a single amplitude, the "projectile excitation" amplitude (when the dashed curve is not visible, it is indistinguishable from the full result). In fact, to good approximation, we could just calculate this single amplitude and obtain results within a few percent of the full calculations. Note that this is markedly different from the results obtained for the $(p,p'\pi)$ reaction,[7] where all four amplitudes gave roughly equal cross sections. The difference between the two reactions is that η production occurs through S-wave π-N amplitudes, whereas π production was dominated by P-wave π-N amplitudes. The P-wave amplitudes gave two additional factors of q/m_π. In amplitudes $B-D$, the meson momenta are very large relative to the pion mass; thus the several factors of meson momentum made these amplitudes very large relative to the projectile excitation term. Their absence in η production means that these amplitudes are negligible relative to projectile excitation.

We have not included effects of the nonlocality of the propagating isobar. Miller and Walker[11] showed that

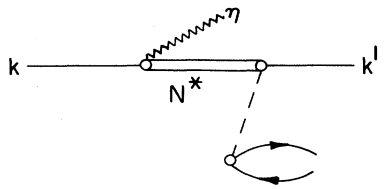

FIG. 6. The crossed diagram contribution to the projectile excitation amplitude of Fig. 2(a). In this amplitude, the η production occurs before the virtual pion is absorbed.

such considerations would likely decrease the contribution from amplitudes $B-D$, while leaving amplitude A essentially unchanged. Thus our qualitative conclusion that η production is dominated by a single amplitude should not change if nonlocality effects are included.

As the projectile excitation amplitude excites only $\Delta T=1$ non-normal-parity transitions, the $(p,p'\eta)$ exclusive reaction should be completely dominated by such transitions. Given the energy and momentum uncertainties inherent in observing the η, it may be quite challenging to demonstrate experimentally this predicted feature of the η-production reaction.

In our calculations, we have neglected the "crossed diagrams," where the η is emitted before the virtual pion is absorbed. Thus we have neglected amplitudes of the form of Fig. 6. In Fig. 7, we show the percent change in the theoretical cross sections when we include the crossed diagram of Fig. 6. We have calculated only the crossed diagram corresponding to the projectile excitation amplitude, since this amplitude completely dominates our theoretical cross sections.

Figure 7 shows the contribution of the crossed diagram, for incident proton energy 1.3 GeV, as a function of the kinetic energy of the outgoing proton. For outgoing energies less than 100 MeV, the crossed diagram contribution is significant. However, as can be seen from Fig. 4, the predicted cross sections in this region are very small. Near the peak of the theoretical cross sections, inclusion of this amplitude makes only a few percent change in the cross sections. We have assumed that the $N^*(1535)$ propagator varies like $W\equiv\sqrt{s}$, as can be seen from Eq. (4); s is the square of the four-momentum of the virtual isobar. For some kinematics, the crossed diagram corresponds to negative values of s, and in this region we have not calculated the correction arising from the crossed diagram. In addition, as we mentioned in Sec. II B, consistent inclusion of the crossed diagrams would involve refitting the amplitude $\pi+N\rightarrow\eta+N$ with these diagrams, and recalculating the coupling constants. As the crossed diagrams give a very small change in our overall results, they have been neglected in the remainder of this work.

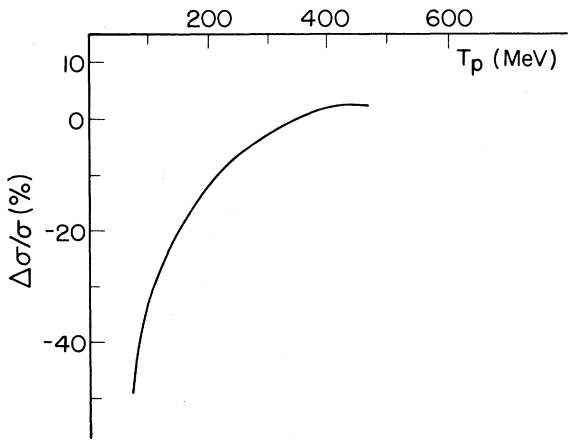

FIG. 7. Percent change in η-production cross sections when crossed diagram of Fig. 6 is added to the amplitudes of Fig. 2. Incident proton energy is 1.3 GeV, and angle θ_η is fixed at $+10°$.

B. Effects of distortions of hadrons

The cross sections calculated in Section III A have not included distortions of the incident or final protons, or the η. We expect that inclusion of distortions should decrease the cross sections by at least an order of magnitude, as inclusion of the absorption occurring from nuclear interactions of the hadrons should decrease each wave function by a factor of roughly 2–3. We would naively expect the proton effects to be considerably greater than the distortion effects from the η, as the theoretical amplitudes of Bhalerao and Liu[6] suggest a rather weak nuclear interaction of the η meson.

For the energies we have considered, both the incoming and outgoing protons, and the outgoing η, tend to have rather large momenta. The largest cross sections come in the vicinity of the $N^*(1535)$ resonance, and also at those regions where the momentum transfer to the nucleus reaches its minimum value. In this kinematic region, the eikonal approximation[12] should give a good estimate of the effects of hadron-nucleus interactions on our predicted cross sections. In the eikonal approximation, one assumes straight-line propagation of the interacting particles. The refraction and absorption effects are calculated by averaging the particle-nucleon forward scattering amplitudes over the nucleon density at each point in space, and adding up the accumulated (complex) phases as the particles traverse the nucleus.

With the eikonal approximation, the nuclear transition densities ρ_{fi} appearing in T_A and T_D from our plane-wave results must be replaced by eikonal distorted-wave transition densities ρ_{fi}^{DW}, where

$$\rho_{fi}^{\mathrm{DW}}(\mathbf{k}_\eta+\mathbf{k}'-\mathbf{k})=\int bdb\,dz\,d\phi\,\rho_{fi}(b,z)\times\exp[-i(\mathbf{k}_\eta+\mathbf{k}'-\mathbf{k})\cdot\mathbf{r}]\times I_N(\mathbf{b},z;\mathbf{k})I_N(\mathbf{b},z;\mathbf{k}')I_\eta(\mathbf{b},z;\mathbf{k}_\eta)\ , \tag{26}$$

with

$$I_N(\mathbf{b},z;\mathbf{k})\equiv\exp\left[-\frac{iE_{\mathbf{k}}}{k}\int_{-\infty}^{z}\langle f_{NN}(k)\rangle\rho_A(\mathbf{b},\hat{k}z')dz'\right],$$

$$I_N(\mathbf{b},z;\mathbf{k}')\equiv\exp\left[-\frac{iE_{\mathbf{k}'}}{k'}\int_{0}^{\infty}\langle f_{NN}(k')\rangle\rho_C(\mathbf{r}+\hat{k}'s)ds\right],$$

$$I_\eta(\mathbf{b},z;\mathbf{k}_\eta)\equiv\exp\left[-\frac{i\omega_\eta}{k_\eta}\int_{0}^{\infty}\langle f_{\eta N}(k_\eta)\rangle\rho_C(\mathbf{r}+\hat{k}_\eta s)ds\right], \tag{27}$$

where $\mathbf{r}\equiv\mathbf{b}+\mathbf{z}$, and ρ_{fi} is the nuclear transition density in coordinate space [i.e., it is the Fourier transform of Eq. (15)]. In Eq. (27), $f_{\eta N}$ and f_{NN} denote, respectively, the energy-dependent forward-angle ηN and NN scattering amplitudes. The brackets $\langle\ \rangle$ denote the isospin-averaged amplitudes for a proton interacting with Z protons and N neutrons in the target and final nuclei; the η-N amplitudes were obtained from Bhalerao and Liu, Ref. 6. The variables $\hat{k}'$ and $\hat{k}_\eta$ appearing in the final nuclear density, ρ_C, indicate that the distortion effects are calculated along the directions $\hat{k}'$ and $\hat{k}_\eta$ of the outgoing proton and η. A detailed derivation of this eikonal form can be found in Ref. 13.

Similarly, in the amplitudes T_B and T_C, the single-particle wave functions ϕ are replaced by the distorted wave functions; for example, we have

$$[\phi_f^{\mathrm{DW}}(\mathbf{k}-\mathbf{k}_\eta-\mathbf{q})]^\dagger=\int bdb\,dz\,d\phi\,\phi_f(\mathbf{r})^\dagger\exp[i(\mathbf{k}-\mathbf{k}_\eta-\mathbf{q})\cdot\mathbf{r}]I_N(b,z;\mathbf{k})I_\eta(b,z;\mathbf{k}_\eta) \tag{28}$$

In deriving these formulas for the eikonal distortions, we have neglected the nonlocality of the pion and isobar propagation. The medium effects on the pion have been taken account of through the pion propagator defined in Eq. (17). Consequently, neglecting the nonlocality of the pion in the eikonal distortions should not introduce appreciable errors into our results. In the present work, we have not included medium modifications of the isobar, for reasons mentioned in Section II B.

In Fig. 8, we show the distorted-wave cross sections for η production, for fixed outgoing proton angle $-10°$ and fixed η angle $+10°$, as a function of the outgoing proton kinetic energy $T_{p'}$. Results are shown for three different incident proton energies. The solid curves are the full distorted-wave results, the dotted curve includes distortions only for the outgoing proton, the dot-dashed curves include distortions for both incident and outgoing protons but plane waves for the η, and the dashed curves are the plane-wave results. As with the PWA results, we find that the full cross sections are completely dominated by the projectile excitation amplitude.

Our distorted-wave results are about a factor of 50 smaller than the PWA cross sections. The predicted effects of the η distortions are rather small; including nuclear distortions of the η decreases the calculated cross sections by roughly a factor of 2. These effects are much smaller than the effects of proton-nucleus interactions.

The qualitative effects of the proton distortions can be understood rather easily. In the eikonal approximation, the asymptotic momentum of the proton can be related to an *effective momentum* k_e, defined through the relation

$$k^2=k_e^2+2M\langle V\rangle\ . \tag{29}$$

In Eq. (29), k is the asymptotic proton momentum and $\langle V\rangle$ is the average optical potential "seen" by the proton. $\langle V\rangle$ has both a real part and a positive imaginary part. In the impulse approximation, the imaginary part will be related to the proton-nucleus total cross sections; these have a minimum for proton energy about 200 MeV, and are slowly increasing for proton energies around 1 GeV. The absorption will cause the distorted wave function to be smaller than the plane-wave amplitude. For proton *KE* less than about 300 MeV, the real part of the proton-nucleus optical potential is negative, correspond-

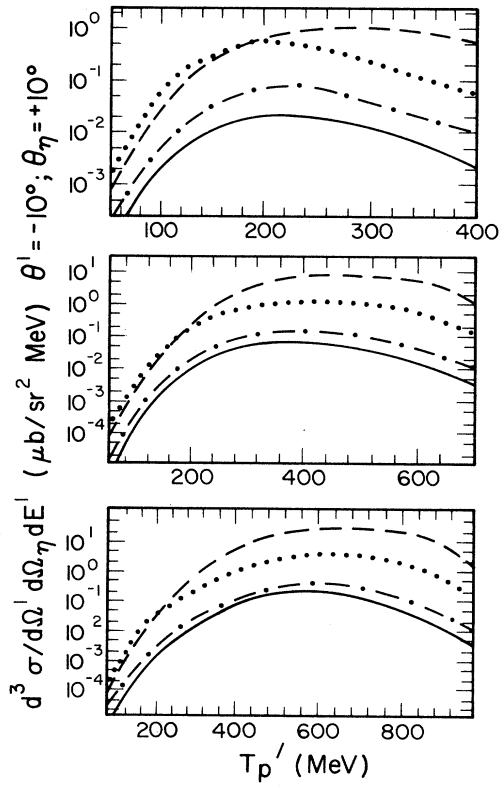

FIG. 8. Same as Fig. 4, with inclusion of nuclear distortions of hadrons through eikonal approximation. Solid curve, full distorted results; dotted curve, distortion only for outgoing proton; dot-dashed curve, distortions for incident and outgoing protons, plane waves for η; dashed curve, PWA for all particles.

ing to an attractive optical potential. As a result, the effective momentum is *larger than* the asymptotic momentum. For proton *KE* greater than 300 MeV, the optical potential is repulsive and the effective momentum k_e is *smaller than* the asymptotic momentum.

From Eq. (A3), we see that the cross sections are governed by the vector q_A defined in Eq. (11). q_A will decrease if the outgoing proton momentum k' is increased. Therefore, from our qualitative arguments regarding the effective momentum, for proton *KE* below (above) 300 MeV, the effective momentum will increase (decrease); thus from these arguments we expect to see an *increase* in the η production cross sections (relative to the PWA results) for very low energies of the outgoing protons, and a progressive decrease of the relative cross sections as the proton *KE* increases. From Fig. 8, this is just what we observe. In fact, for the lowest energies of the outgoing protons, the distorted-wave results (including only the distortions of the outgoing proton) are actually *larger than* the PWA results.

Another factor which contributes to the qualitative behavior of our results, is that the reaction is a high-momentum-transfer process. As a result, we are always in a region where the nuclear transition density is rather small and where it varies rapidly with even small changes in the momentum transfer. Thus even the relatively small shifts in the effective momentum, given approximately by Eq. (29), make significant changes in the numerical results. Note that our approximating the nuclear transition density by a Gaussian probably overemphasizes this effect, as realistic transition densities at large momentum transfers are unlikely to vary as rapidly as the Gaussian.

IV. CONCLUSIONS AND FUTURE OUTLOOK

We have calculated cross sections for exclusive η production from proton bombardment of nuclear targets. Including distortions of the hadrons, we find that predicted peak cross sections depend strongly on the proton incident kinetic energy; peak cross sections increase rapidly as the proton energy increases. This is because the nuclear momentum transfer decreases as the proton energy increases.

The cross sections are dominated by a single amplitude: the "direct projectile excitation" amplitude. The contribution from all other amplitudes, and from the crossed amplitude, are much smaller than this amplitude. We showed that this is due to the fact that the $N^*(1535)$ is an S-wave π-N resonance. Since only a single term dominates the cross sections, it should excite only non-normal-parity $\Delta T=1$ nuclear states.

Including the effects of distortions, we predict peak cross sections of the order of 1 μb/sr^2 MeV. In Fig. 9, we plot the theoretical peak distorted-wave cross sections as a function of incident proton energy. Note that at 800 MeV we predict peak cross sections of only 1 nb/sr^2 MeV. Note that our calculations do not include explicit many-body effects. These may be of considerable importance, as suggested by two experiments.

The first experiment is the recent measurement of the process $d+p\rightarrow{}^3\mathrm{He}+\eta$ at Saturne.[3] These measurements, taken just above the threshold for η production, showed surprisingly large cross sections, as large as those for π^0 near threshold.[14] These large cross sections have been interpreted by Laget and Lecolley[4] as evidence for very important many-body effects in η production. They claim that the dominant η-production process in this reaction involves resonant rescattering of the virtual pion from the third nucleon; they claim that this process produces cross sections more than two orders of magnitude larger than the results from the direct two-body process considered in this paper.

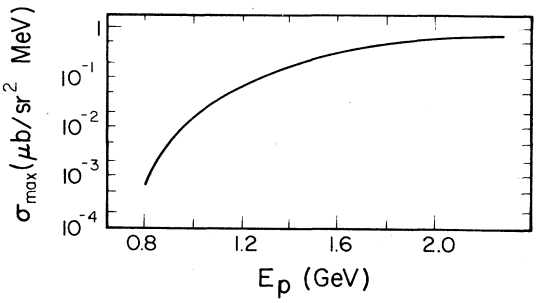

FIG. 9. Peak differential cross sections for $(p,p'\eta)$ reaction on ^{16}O, in μb/sr^2 MeV, vs incident proton *KE* in GeV.

The second experiment which suggests large enhancements to simple production mechanisms is η photoproduction on the deuteron.[15] The experimental results are significantly larger than the most recent theoretical calculation by Halderson and Rosenthal.[16] Here the cause of the discrepancy is not so clear, as earlier theoretical calculations gave results much closer to experiment.[17] However, it also suggests that η-production cross sections may be much larger than predicted by the simplest theoretical models involving a two-body mechanism proceeding through the $S_{11}(1535)$ isobar.

In connection with the recent threshold production of η in $d+p$ reactions, we have included isobar-hole terms in the pion self-energy, which should take into account some of the reaction mechanism of Laget and Lecolley. Nevertheless, if their arguments are correct, then it is quite possible that our theoretical predictions will far underestimate experimental η production cross sections at rather low energies. It might therefore be useful to make even crude experimental measurements of η production on nuclei.

ACKNOWLEDGMENTS

Some of the work reported in this paper was carried out when one of the authors (L.C.L.) was visiting the Indiana University Nuclear Theory Center and Cyclotron Facility. He acknowledges the financial support and hospitality provided to him during these visits. Also, two of the authors (J.T.L. and G.E.W.) thank the Clinton P. Anderson Meson Physics Facility (LAMPF) for their support during visits there, where some of this work was done. The research was supported in part by the U.S. National Science Foundation under Contract No. NSF-PHY88-805640.

APPENDIX: PLANE-WAVE REACTION CROSS SECTIONS

The amplitudes for the $(p,p'\eta)$ reaction proceeding via an intermediate $N(1535)$ state give rise to four terms, shown diagrammatically in Figs. 2(a)–(2(d). The c.m. differential cross section is given in terms of the amplitudes as

$$\frac{d^3\sigma}{d\Omega' d\Omega_\eta dE'} = \frac{10^4}{2(2\pi)^5}\frac{k' k_\eta E' E}{k(1+E/E_A)}|T_{fi}|^2 . \quad \text{(A1)}$$

In Eq. (A1), the units are μb/sr^2 MeV, and $|T_{fi}|^2$ is obtained by squaring the amplitudes of Eqs. (10), (18), (20), and (22), averaging over initial spins and summing over final spins. The cross sections are calculated for an unpolarized incident proton. In this appendix, we neglect the distortion of the incident and outgoing hadrons; eikonal distortions are included in Section III B. The reaction is assumed to take place between the projectile proton and a single "active" nucleon in the nucleus, producing a continuum proton and a particle-hole nuclear state. With the simple Gaussian wave functions of Eqs. (14) and (15), the plane-wave-approximation cross sections in this model can be reduced to a sum of terms requiring no more than a single integral. These terms are listed in the following equations.

The square of the transition amplitude can be written as a sum of eight terms:

$$|T_{fi}|^2 = c_\tau^2(|T_A|^2+|T_D|^2)+(c'_\tau)^2(|T_B|^2+|T_C|^2) + c_\tau c'_\tau(T_{AB}+T_{AC}+T_{BD}+T_{CD}) . \quad \text{(A2)}$$

Equation (A2) defines the cross sections for transitions to final nuclear states with isospin τ; the coefficients c_τ and c'_τ are defined in Eqs. (10) and (18). In general, there will be two additional interference terms, T_{AD} and T_{BC}. However, these terms vanish when spin-averaged.

The first amplitude corresponds to emission of a virtual pion from a target nucleon, excitation of the incident proton of momentum $\mathbf{k}$ to an $N(1535)$ isobar, with subsequent decay to a continuum proton and η, with momenta $\mathbf{k}'$ and $\mathbf{k}_\eta$, respectively. This amplitude is referred to either as the "projectile excitation" term, or alternatively as "amplitude A" [referring to the diagram of Fig. 2(a)]. The equation for this amplitude in PWA is given in Eq. (10). In this equation, the nuclear transition density is taken from Eqs. (13) and (15); the intermediate pion propagator from Eq. (17); the isobar propagator from Eq. (4); and the form factors from Eqs. (7), (8), and (6). In plane-wave approximation, this amplitude gives the contribution

$$|T_A|^2 = cH(q_A)^2 \exp\left[\frac{-q_A^2}{2p_0^2}\right]\frac{q_A^2}{|D_A^* D_A^\pi|^2} , \quad \text{(A3)}$$

where the coefficient c is common to every term, defined as

$$c \equiv 2\left[\frac{f_\pi f^* f_\eta}{m_\pi}\right]^2 . \quad \text{(A4)}$$

One additional amplitude requires no integration in the PWA; this amplitude is obtained by exchanging the bound and continuum nucleon lines in the final state of the "target excitation" amplitude. This term, shown in Fig. 2(d) and called "amplitude D," is given in Eq. (22). Its plane-wave value has the form

$$|T_D|^2 = cH(q_D)^2 \exp\left[\frac{-q_A^2}{2p_0^2}\right]\frac{q_D^2}{|D_D^* D_D^\pi|^2} . \quad \text{(A5)}$$

The next term corresponds to emission of a pion by the projectile proton, as shown in Fig. 1(b). This pion excites a target nucleon to an $N^*(1535)$, which then decays to the final continuum proton and η. This amplitude, the target excitation term, or "amplitude B," is given in Eq. (18), and in PWA has the form

$$|T_B|^2 = c|a_B|^2|I_2|^2 , \quad \text{(A6)}$$

where

$$a_B = \frac{4}{\sqrt{\pi} p_0 R D^*(\omega_B^*)} \exp\{-[k^2+(\mathbf{k}'+\mathbf{k}_\eta)^2]/2p_0^2\} , \quad \text{(A7)}$$

and

$$I_2 = \int_0^\infty \frac{dq\, q^2 \exp(-q^2/p_0^2) H_B(q)}{D_\pi(q,\omega_B)} \times[\cosh(u)-\sinh(u)/u] , \quad \text{(A8)}$$

where

$$u \equiv \frac{qR}{p_0^2} , \quad \text{(A9)}$$

and the vector $\mathbf{R}$ appearing in Eq. (A9) is defined by

$$\mathbf{R} \equiv \mathbf{k}+\mathbf{k}'+\mathbf{k}_\eta . \quad \text{(A10)}$$

The final amplitude, given in Fig. 2(c), referred to as "amplitude C," is obtained from amplitude A by exchanging the continuum and bound nucleon lines in the final state. In PWA, $|T_C|^2$ is identical in form to the term $|T_B|^2$; it is given by

$$|T_C|^2 = c|a_C|^2|\tilde{I}_2|^2 . \quad \text{(A11)}$$

In Eq. (A11), $\tilde{I}_2$ is obtained from I_2 of Eq. (A8) by the substitutions

$$\omega_B \to \omega_C , \quad H_B(q) \to H_C(q) , \quad \mathbf{R} \to \mathbf{R}' , \quad \text{(A12)}$$

where $\mathbf{R}'$ is defined by

$$\mathbf{R}' \equiv \mathbf{k}+\mathbf{k}'-\mathbf{k}_\eta . \quad \text{(A13)}$$

The overall coefficient a_C in Eq. (A11) is defined by

$$a_C = \frac{4}{\sqrt{\pi} p_0 R' D^*(\omega_C^*)} \exp\{-[k'^2+(\mathbf{k}-\mathbf{k}_\eta)^2]/2p_0^2\} . \quad \text{(A14)}$$

The interference term T_{AB} can be defined as

$$T_{AB} = -c \exp\left[\frac{-q_A^2}{2p_0^2}\right] q_A \cos\tilde{\theta}_A \mathrm{Re}\left[\frac{(a_B I_2)^\dagger}{D_A^* D_A^\pi}\right], \quad \text{(A15)}$$

where a_B and I_2 are given in Eq. (A8). In Eq. (A15), the angle $\tilde{\theta}_A$ is the angle between the vectors $\mathbf{q}_A$ and $\mathbf{R}$, defined in Eqs. (11) and (A10), respectively.

The interference term T_{AC} is identical in form to the term T_{AB}, if every term in Eqs. (A7) and (A8) is converted to the appropriate terms defined in Eqs. (A12) and (A14) (and the angle $\tilde{\theta}_A$ is replaced by the angle between the vectors $\mathbf{q}_A$ and $\mathbf{R}'$).

The interference term T_{BD} is given by

$$T_{BD} = -c \exp\left[\frac{-q_A^2}{2p_0^2}\right] q_D \cos\tilde{\theta}_D \mathrm{Re}\left[\frac{(a_B I_2)^\dagger}{D_D^* D_D^\pi}\right]. \quad \text{(A16)}$$

The interference term T_{CD} is identical in form to the term T_{BD}, if every term in Eq. (A16) is converted to the appropriate terms defined in Eqs. (A12) and (A14).

[1]Review of particle properties, Phys. Lett. **170B**, 1 (1986).
[2]Q. Haider and L. C. Liu, Phys. Lett. B **172**, 257 (1986); **174**, 465 465(E) (1986); L. C. Liu and Q. Haider, Phys. Rev. C **34**, 1845 (1986).
[3]J. Berger *et al.*, Phys. Rev. Lett. **61**, 919 (1988).
[4]J. M. Laget and J. F. Lecolley, Phys. Rev. Lett. **61**, 2069 (1988).
[5]L. C. Liu (unpublished).
[6]R. S. Bhalerao and L. C. Liu, Phys. Rev. Lett. **54**, 865 (1985).
[7]B. K. Jain, J. T. Londergan, and G. E. Walker, Phys. Rev. C **37**, 1564 (1988).
[8]D. J. Herndon *et al.*, Lawrence Berkeley Laboratory Report No. UCRL-20030 πN (unpublished).
[9]R. M. Brown *et al.*, Nucl. Phys. **B153**, 89 (1979).
[10]M. Hirata, J. H. Koch, F. Lenz, and E. J. Moniz, Ann. Phys. (N.Y.) **120**, 205 (1979); E. Oset, H. Toki, and W. Weise, Phys. Rep. **83**, 282 (1982).
[11]G. A. Miller and G. E. Walker, Phys. Lett. **106B**, 358 (1981).
[12]R. J. Glauber, in *Lectures in Theoretical Physics,* edited by W. E. Brittin (Interscience, New York, 1959), Vol. 1, p. 315; in *High Energy Physics and Nuclear Structure,* edited by G. Alexander (North-Holland, Amsterdam, 1967), p. 311.
[13]Y. Ohkubo and L. C. Liu, Phys. Rev. C **30**, 254 (1984).
[14]M. A. Pickar, in *Pion Production and Absorption in Nuclei–1981,* Proceedings of the Conference on Pion Production and Absorption in Nuclei, edited by R. D. Bent, AIP Conf. Proc. No. 79 (AIP, New York, 1982).
[15]R. L. Anderson and R. Prepost, Phys. Rev. Lett. **23**, 46 (1969).
[16]D. Halderson and A. S. Rosenthal (unpublished).
[17]N. Hoshi, H. Hyuga, and K. Kubodera, Nucl. Phys. **A324**, 234 (1979).